JOURNAL OF PLANKTON RESEARCH | VOLUME 27 | NUMBER 2 | PAGES 189–197 | 2005

SHORT COMMUNICATION

Seasonal and interannual variability of chlorophyll *a* and primary production in the Equatorial Atlantic: *in situ* and remote sensing observations

VALESCA PÉREZ[1]*, EMILIO FERNÁNDEZ[1], EMILIO MARAÑÓN[1], PABLO SERRET[1] AND CARLOS GARCÍA-SOTO[2]

[1]FACULTAD DE CIENCIAS DEL MAR, UNIVERSIDAD DE VIGO, E-36310 VIGO, SPAIN AND [2]INSTITUTO ESPAÑOL DE OCEANOGRAFÍA, CENTRO OCEANOGRÁFICO DE SANTANDER, APDO 240, E-39080 SANTANDER, SPAIN

*CORRESPONDING AUTHOR: vperez@uvigo.es

Received July 19, 2004; accepted in principle September 17, 2004; accepted for publication October 28, 2004; published online November 22, 2004

The seasonal variability of phytoplankton in the Equatorial Atlantic was analysed using Sea-viewing Wide Field-of-view Sensor (SeaWiFS)-derived chlorophyll a (Chl a) concentration data from 1998 to 2001, together with in situ Chl a and primary production data obtained during seven cruises carried out between 1995 and 2000. Monthly averaged SeaWiFS Chl a distributions were in agreement with previous observations in the Equatorial Atlantic, showing marked differences between 10° W in the Eastern Tropical Atlantic (ETRA) and 25° W in the Western Tropical Atlantic (WTRA) provinces (Longhurst et al. 1995. J. Plankton Res., 17, 1245–1271). The seasonal cycle of SeaWiFS-derived Chl a concentration calculated for 0–10° S, 0–20° W (ETRA) is consistent with in situ Chl a measurements, with values ranging from 0.16 mg m^{-3}, from February to April, to 0.52 mg m^{-3} in August. Lower variability was observed in 10° N–10° S, 20–30° W (WTRA) where minimum and maximum concentrations occurred in April (0.15 mg m^{-3}) and in August (0.24 mg m^{-3}), respectively. A significant empirical relationship between depth-integrated primary production and in situ measured sea surface Chl a was found for ETRA, allowing us to estimate the seasonal cycle of depth-integrated primary production from SeaWiFS-derived Chl a. As for Chl a, this model was verified in a small area of the Eastern Equatorial Atlantic (0–10° S, 0–20° W), although in this instance it was not completely able to describe the magnitude and temporal variability of in situ primary production measurements. The annual euphotic depth-integrated primary production rate estimated for ETRA by our empirical model was 1.4 Gt C $year^{-1}$, which represents 16% of the open ocean primary production estimated for the whole Atlantic Ocean.

INTRODUCTION

The Sea-viewing Wide Field-of-view Sensor (SeaWiFS) images have generated an unprecedented data set in terms of coverage, continuity and duration allowing the observation of phytoplankton spatial, seasonal and interannual variability (Gregg, 2002). This information, together with earlier data provided by the Coastal Zone Color Scanner (CZCS), has revealed the existence of large variations in sea surface chlorophyll *a* (Chl *a*) concentration in the Equatorial Atlantic over seasonal scales (Longhurst, 1993; McClain and Firestone, 1993; Yoder *et al.*, 1993; Longhurst *et al.*, 1995; Rudjakov, 1997; Signorini *et al.*, 1999). The magnitude of phytoplankton blooms observed in this oceanic region, which

doi:10.1093/plankt/fbh159, available online at www.plankt.oupjournals.org

has been compared in terms of primary production to the North Atlantic spring bloom (Platt *et al.*, 1991), illustrates the significance of the Equatorial Atlantic for the carbon budget of the Atlantic Ocean.

Recurrent phytoplankton blooms typically occur in the eastern Tropical Atlantic during boreal summer, although their onset and duration is subject to interannual variability (Signorini *et al.*, 1999) associated with the seasonal meridional displacement of the Intertropical Convergence Zone (ITCZ). The northward migration of the ITCZ during boreal summer and the subsequent intensification of the southeast trade winds causes a seasonal adjustment of the thermocline, which gets deeper in the western basin while shoaling in the eastern basin. As a consequence of this upward displacement, both the thermocline and the upper mixed layer are shallower in the eastern Tropical Atlantic. The pivot line of this basin-scale movement is centred at 15–20° W. When the ITCZ moves southward and the trade winds become weak (in the early months of the year), differences in thermocline depth between both basins tend to disappear.

The seasonal variations observed in sea surface Chl *a* and in the surface thermal conditions are also detected in other biological variables. Early measurements in the Equatorial Atlantic suggested the existence of a considerable degree of seasonal variability in primary production, at least in the Gulf of Guinea (Herbland *et al.*, 1983). In this region, the year is divided into two seasons (Herbland and Le Bouteiller, 1982): the cold season (from June to October), when the active equatorial upwelling injects nutrients into the upper mixed layer leading to surface Chl *a* and primary production maxima; and the warm season (from October to May), when the Equatorial Atlantic is characterized by the Typical Tropical Structure (TTS) (Herbland and Voituriez, 1979), where a low Chl *a*, nutrient-depleted upper mixed layer is separated by a strong thermocline from the nutrient-rich, lower layer. In the TTS, Chl *a* and primary production maxima are located close to the thermocline.

Despite the seasonality observed in hydrodynamic conditions and sea surface Chl *a*, conflicting reports exist on the seasonal changes in depth-integrated Chl *a* and primary production rates in the Equatorial Atlantic. Bauerfeind (Bauerfeind, 1987) found higher depth-integrated primary production rates when the equatorial upwelling injected nutrients into the euphotic layer at 22° W. On the contrary, Herbland *et al.* (Herbland *et al.*, 1987) suggested that in the eastern Equatorial Atlantic the seasonal upwelling only results in an upward displacement of the Chl *a* and primary production maxima, without actually changing the magnitude of the total, depth-integrated Chl *a* concentration and primary production rate. Previous studies (Herbland *et al.*, 1983) suggested that the lack of seasonal variability in the depth-integrated values of the above mentioned variables was the result of the strong control of primary producers by zooplankton grazing, as reported for this area by Le Borgne (Le Borgne, 1981).

In this study, we used recent data obtained from seven cruises carried out in the Equatorial Atlantic between 1995 and 2000, as part of the Atlantic Meridional Transect (AMT) programme (Aiken *et al.*, 2000), and SeaWiFS-derived data in order to further explore the seasonal variability in phytoplankton dynamics in the Equatorial Atlantic and to assess whether the seasonal equatorial upwelling does modify phytoplankton standing stocks and productivity.

METHOD

Remote sensing observations

The SeaWiFS data presented in this study were processed at Instituto Español de Oceanografia (IEO) using global monthly Level 3 files provided by the NASA Goddard Space Flight Center (GSFC) Distributed Active Archive Center (DAAC). The files were selected for the period January 1998 to December 2001 (48 monthly files) so as to cover four complete years during a period relatively near the AMT cruises used in this study (1995–2000). The initial NASA data had a bin resolution of ~0,088° of latitude and longitude. The equatorial region of each file was subsampled and converted to SeaWiFS Chl *a* concentration (mg Chl *a* m^{-3}) excluding the values blanked at GSFC DAAC. These blank values represent the presence of land, cloud, sunglint and coccolithophore blooms (Garcia-Soto *et al.*, 1995, 1996) among other excluding factors. The general Chl *a* environment in the Equatorial Atlantic (10° N–10° S) was inspected for a particular year (2001) using monthly SeaWiFS Chl *a* images of the SeaWiFS Project. In order to analyse the differences between the ETRA and WTRA provinces (Longhurst *et al.*, 1995), we chose two locations at the Equator (10 and 25° W) close to the AMT cruise tracks. The term province in this study is used as defined by Longhurst *et al.* (Longhurst *et al.*, 1995). The data for the annual cycles at these locations were averaged in a region of 1° latitude × 1° longitude. SeaWiFS Chl *a* data were also averaged over a larger extension, 30-20° W, 10° N–10° S (WTRA) and 20–0° W, 0-10° S (ETRA), in comparison with *in situ* measurements (Fig. 1).

The seasonality of the equatorial sea surface temperature (SST) was also inspected for the same regions (ETRA, 10° W and WTRA, 25° W) and years (January

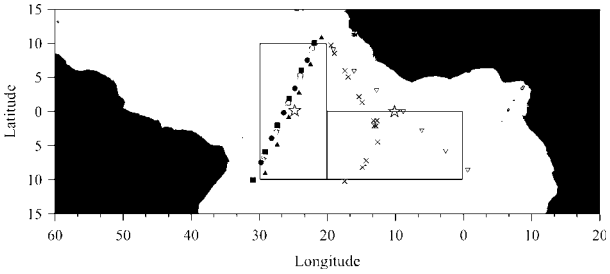

Fig. 1. Map showing the location of Atlantic Meridional Transect (AMT) stations in the Equatorial Atlantic from 10° N to 10° S: AMT-1 (○), AMT-2 (●), AMT-3 (□), AMT-4 (■), AMT-5 (▲), AMT-6 (▽) and AMT-11 (x); black boxes represent the areas where SeaWiFS-derived chlorophyll *a* was averaged and from which National Oceanographic Data Center (NODC) data were obtained, and stars indicate two representative locations (10 and 25° W) in the vicinity of the AMT track. See text for details.

1998 to December 2001) in order to analyse the sea surface cooling signal associated with the equatorial upwelling and its relationship with the phytoplankton seasonal signal. The monthly SST data (°C) used were extracted from a public data base of the National Oceanic and Atmospheric Administration (NOAA) Climate Diagnostic Centre (CDC; NOAA OI SST V2 archive; 1 × 1° resolution).

In situ observations

In situ measurements used in this study are restricted to the Equatorial Atlantic (10° N–10° S) and were obtained from several sources.

In situ Chl *a* data corresponding to the defined region were obtained from the National Oceanographic Data Center (NODC) and also from seven cruises conducted on board *RRS James Clark Ross* along large scale latitudinal transects as part of the AMT research programme between 1995 and 2000. Most of the surface (0–10 m) Chl *a* data were obtained from the World Ocean Atlas Online of the NODC (http://www.nodc.noaa.gov/OC5/WOD01/pr_wod01.html). We used Ocean Station Data (OSD) corresponding to the World Meteorological Organization (WMO) squares 5000, 5001, 5002 and 7002 which are close to the AMT cruise tracks although they do not cover the whole extension of ETRA and WTRA provinces as defined by Longhurst *et al.* (Longhurst *et al.*, 1995). The total number of observations of Chl *a* concentration in the squares belonging to the ETRA and WTRA provinces was 401 and 534, respectively, most of them collected in the July to August and January to February periods. Stations with anomalously high (>4 mg m^{-3}) Chl *a* values (three stations located in the WTRA province sampled in autumn 1981) were excluded from the analysis. Observations were monthly averaged in order to construct a seasonal cycle. Fluorometrically measured Chl *a* concentrations from AMT-1, AMT-2, AMT-3, AMT-4 and AMT-5 were taken from Marañón *et al.* (Marañón *et al.*, 2000, 2001), AMT-6 data from Serret *et al.* (Serret *et al.*, 2001) and AMT-11 from Serret *et al.* (Serret *et al.*, 2002).

The protocol used to determine primary production using ^{14}C-uptake experiments during the AMT cruises has been previously described (Marañón *et al.*, 2000). Hourly primary production rates were converted to daily rates by taking into account the incident irradiance (PAR) integrated both throughout the incubation and the daylight time periods, except for the AMT-4 and AMT-6 data set when, due to the unavailability of PAR data, we used daylight lengths calculated from the equation by Straskraba and Gnauck (Straskraba and Gnauck, 1985). In addition, dark respiration losses were considered to account for 20% of the light ^{14}C incorporation (Marañón *et al.*, 2000, and references therein). Depth-integrated primary production data were also taken from the literature. In particular, we used the data set presented in Herbland *et al.* (Herbland *et al.*, 1983) who refers to data previously measured between 1° N and 5° S at 5 and 10° W in 1963–65 (Tchmir, 1971).

RESULTS AND DISCUSSION

Spatial and seasonal variability in Chl *a* concentration

Figure 2 shows monthly SeaWiFS Chl *a* composites in the Equatorial Atlantic from January to December 2001. The main features observed in the surface Chl *a* distributions are related to the Congo and Amazon river plumes, the equatorial upwelling and the coastal upwelling off north west (NW) and south west (SW) Africa. High Chl *a* values were detected in the Amazon and Congo river deltas (5–10 mg m^{-3}) throughout the year. The Congo river plume reached its maximum extent and Chl *a* concentration from May to September coinciding with the development of the Chl *a* maximum offshore. During most of the year, Amazon water was carried into the Caribbean Sea by the North Brazil Current (NBC), as observed from the river plume (Chl *a* concentrations ranging from 0.5 to 5 mg m^{-3}) that reaches its maximum northward spread in June to July. From August to December, Amazon water was introduced in the equatorial circulation system because of the retroflection of the NBC at 5° N and contributed to the North Equatorial Countercurrent (NECC). The offshore Equatorial Atlantic showed low Chl *a* levels (<0.2 mg m^{-3}) from February to April. In June, a Chl *a* filament (>0.5 mg Chl m^{-3}) was observed along the Equator from the African coast to ~20° W. In August, Chl *a*

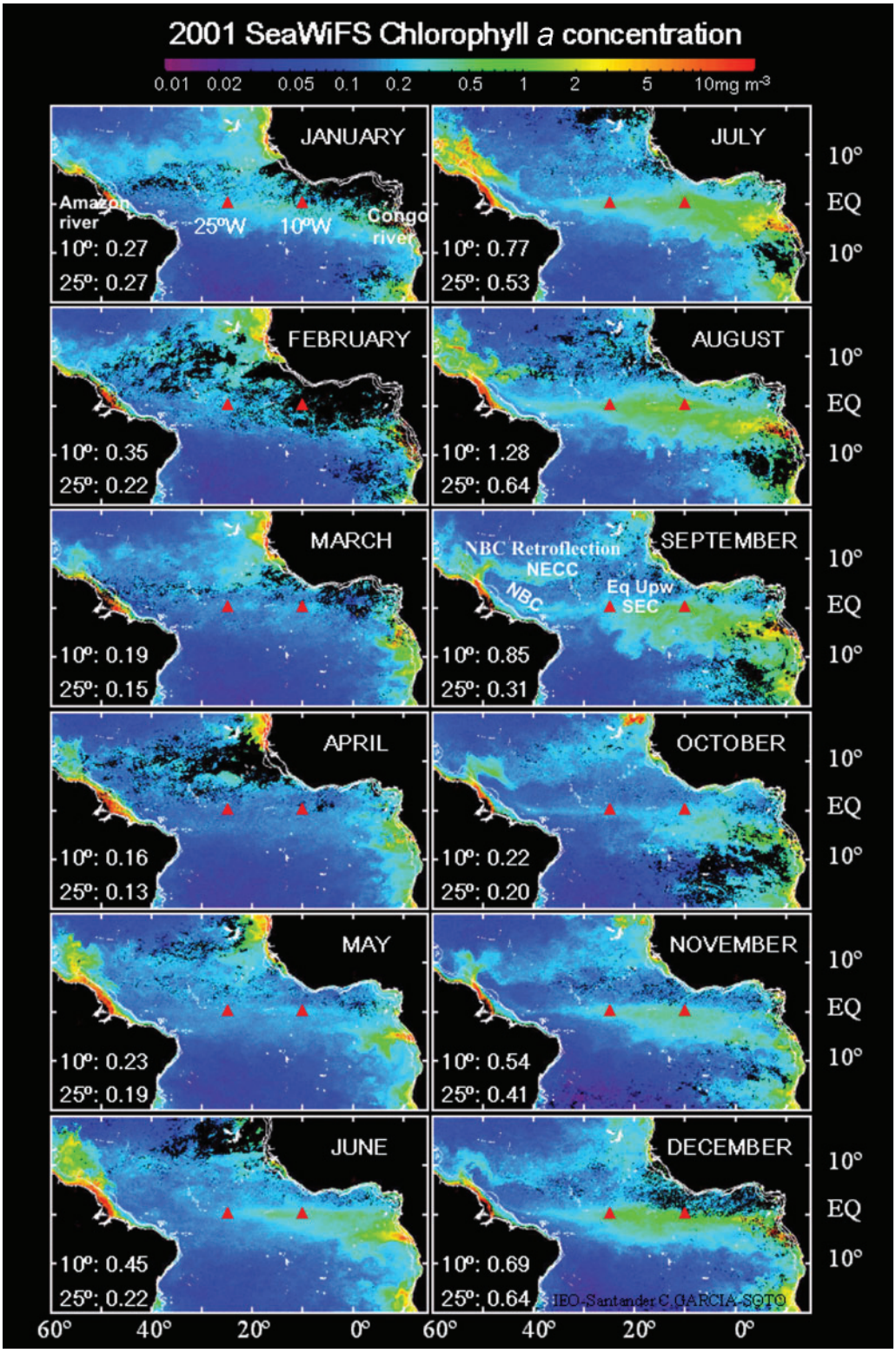

Fig. 2. Monthly composite maps of Sea-viewing Wide Field-of-view Sensor (SeaWiFS) chlorophyll *a* (Chl *a*) concentration (mg m^{-3}) in the Equatorial Atlantic for 2001. SeaWiFS Chl *a* values (1° × 1° bins; mg m^{-3}) from NASA Distributed Active Archive Centre (DAAC) for those two locations are given in the bottom left corner of each panel.

concentration in this filament increased, reaching values >2 mg m^{-3}, and extended westward to the Brazil coast and southward to 10° S. The bloom receded in September to strengthen again in November along the Equator. High Chl *a* concentrations were observed in the NW and SW coast of Africa during most of the year. These observations are similar to those previously reported by Longhurst (Longhurst, 1993) and Monger *et al.* (Monger *et al.*, 1997). In contrast, Signorini *et al.* (Signorini *et al.*, 1999) described a Chl *a* maximum in August and low Chl *a* concentrations in December as a consequence of an anomalous response of the upper ocean to changes in the wind field associated with El Niño 1997–98.

The data set presented in Fig. 2 also allows to visualize the differences in the spatial and temporal variability of surface Chl *a* between the eastern and the western Equatorial Atlantic in 2001. To this aim, two locations along the Equator at 10 and 25° W, represented in the Fig. 2 by red triangles, were selected to illustrate the Chl *a* variability in the ETRA and WTRA provinces. Chl *a* values at 25° W ranged from 0.13 to 0.64 mg m^{-3} and were somewhat less variable than those obtained at 10° W (0.16–1.28 mg m^{-3}). The highest Chl *a* values at 25° W were reached in July to September coinciding with the maximum extension and magnitude of the equatorial phytoplankton bloom which, in general, had been previously initiated in the eastern Equatorial Atlantic. During this period, high differences in Chl *a* values between 10° W (ETRA) and 25° W (WTRA) were observed, being quite similar during the rest of the year. The monthly averaged values of SeaWiFS Chl *a* obtained at 25 and 10° W from January 1998 to December 2001 (Fig. 3A) indicate that the seasonal pattern observed in 2001 is representative of the Chl *a* seasonality of this region except during November and December when Chl *a* concentrations were much higher than in precedent years. In general, higher monthly averaged Chl *a* concentrations at 10° W (ETRA) were reached in August and December with values ranging from 0.66 mg m^{-3} in 1998 to 1.28 mg m^{-3} in 2001 during boreal summer and from 0.42 mg m^{-3} in 1998 to 0.69 mg m^{-3} in 2001 during boreal winter. An exception to this pattern occurred in 2000 when the boreal summer Chl *a* maximum took place in June to July. Minimum Chl *a* values in spring and fall (around 0.2 mg m^{-3}) were observed in the 4 years. At 25° W (WTRA), the annual cycles of SeaWiFS monthly averaged Chl *a* showed lower annual variability and lower values (ranging from 0.1 to 0.8 mg m^{-3}) than at 10° W (ETRA). Chl *a* maxima at 25° W (WTRA) were found in July to August and December coinciding with periods of maximum Chl *a* concentrations at 10° W (ETRA). An exceptional situation was found during the summer bloom observed at 25° W (WTRA) in 1999 when Chl *a* concentrations reached the highest value

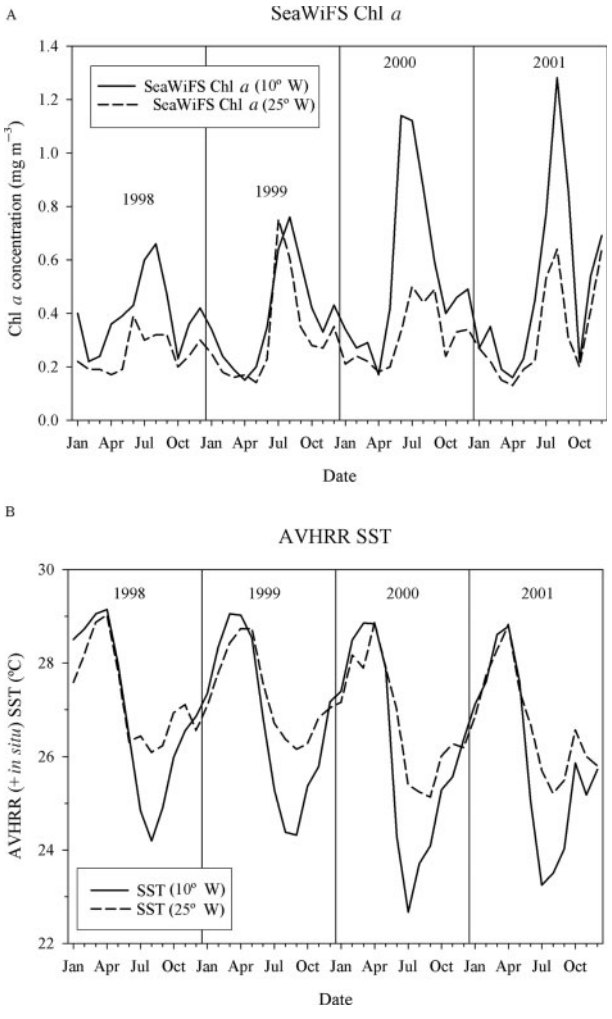

Fig. 3. (**A**) Sea-viewing Wide Field-of-view Sensor chlorophyll *a* (SeaWiFS Chl *a*) concentration (mg m^{-3}) at the Equator at 10° W (ETRA region; solid line) and 25° W (WTRA region; dashed line). The data, provided by NASA Distributed Active Archive Centre (DAAC), were averaged in bins of 1° latitude × 1° longitude at monthly intervals for the period January 1998 to December 2001. (**B**) Monthly values of sea surface temperature (SST; °C) for the same locations (ETRA at 0° N/S, 10° W and WTRA at 0° N/S, 25° W) and time interval (January 1998 to December 2001). The SST data were provided by the NOAA Climate Diagnostic Center (CDC; NOAA OI SST V2 archive; 1° × 1° resolution).

(0.8 mg m^{-3}) recorded during the 4-year period, which were of similar magnitude to those measured at 10° W (ETRA). In both locations the seasonal Chl *a* variability was higher than interannual variations.

Seasonal cooling of surface waters and associated nutrient enrichment of the euphotic layer during the boreal summer has been described extensively in the literature (Oudot, 1983; Colin *et al.*, 1987; Hastenrath and Merle, 1987; Oudot and Morin, 1987; Carton and Zhou, 1997). In this study, changes in SST mirrored those of Chl *a* concentration estimated from SeaWiFS both at 10° W (ETRA) and at 25° W (WTRA) (Fig. 3B).

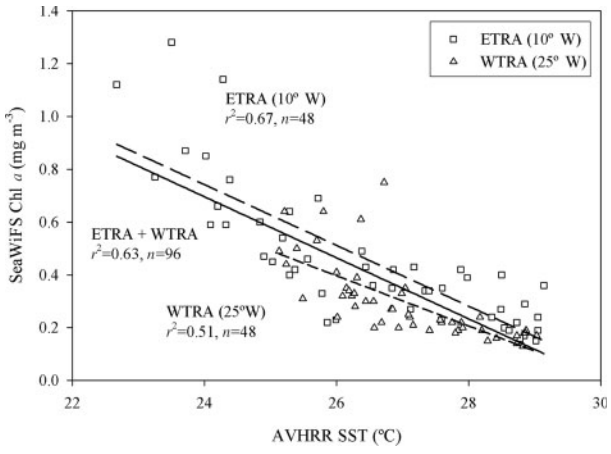

Fig. 4. Empirical relationship between Sea-viewing Wide Field-of-view Sensor chlorophyll *a* (SeaWiFS Chl *a*) concentration (mg m^{-3}) and Advanced very High Resolution Radiometer sea surface temperature (AVHRR SST) (°C) obtained from 1998 to 2001 at 10° W in ETRA (squares) and at 25° W in WTRA (triangles) provinces. Long and short dashed line represent the linear relationship between both variables at 10° W (ETRA) and at 25° W (WTRA), respectively, whereas the solid line represents the relationship using all available data at 10 and 25° W (ETRA + WTRA).

A significant linear relationship (Fig. 4) was obtained between both variables at 10° W (Chl a = 3.50–0.12 SST, $r^2 = 0.67$, $n = 48$, $P < 0.0001$) and 25° W (Chl a = 2.87–0.10 SST, $r^2 = 0.51$, $n = 48$, $P < 0.0001$) and when both data sets were pooled together (Chl a = 3.47–0.12 SST, $r^2 = 0.63$, $n = 96$, $P < 0.0001$). This inverse correlation was already highlighted by Longhurst (Longhurst, 1993) who suggested that the spatial and temporal coincidence of SST cooling and phytoplankton blooms in the Equatorial Atlantic allows an inference of the mechanisms behind the induction of the outbursts of phytoplankton biomass in this area. During boreal summer, the intensification of the SE trade winds, which affects mainly the western basin of the Equatorial Atlantic, makes the thermocline shoal in the eastern basin while deepening it in the western basin. At the same time, the increase of local winds in the eastern region induces the entry of cool, nutrient-rich waters into the surface, initiating a phytoplankton bloom that consumes the upwelled nitrate down to a depth where light becomes limiting. In this hydrodynamic scenario, maximum Chl *a* concentrations are located close to the surface (Herbland *et al.*, 1983). However, this is not the only mechanism proposed to explain the cooling and the nutrient enrichment of the euphotic layer in the eastern Equatorial Atlantic. Other processes such as the vertical mixing between the South Equatorial Current (SEC) and the Equatorial Undercurrent (EU) and changes in the relative position of the thermocline to the EU with the trade winds or zonal nitrate advection have been also suggested to explain the duration or intensity of phytoplankton blooms in this area (Colin *et al.*, 1987; Monger *et al.*, 1997; Loukos and Mémery, 1999). The combined effect of these processes could account not only for the SST cooling in the eastern Equatorial Atlantic during boreal-summer-fall and the associated sea surface Chl *a* increase detected by remote colour sensors but could also explain, together with the complex equatorial current system, the differences observed between ETRA and WTRA provinces and the spatial development of the phytoplankton bloom. Differences between both provinces and year-to-year variability are also related to variations in global atmospheric circulation (Vinogradow, 1988).

Figure 5 shows the seasonal evolution of cruise averaged surface Chl *a* concentrations measured during the AMT cruises and obtained from the NODC data set in the 10° N–10° S region. Measured values are superimposed to the monthly mean SeaWiFS Chl *a* concentration averaged for 10° N–10° S, 20–30° W (WTRA) and 0–10° S, 20–0°W (ETRA) over the 1998–2001 period (see Methods). In ETRA (Fig. 5A) *in situ* Chl *a* concentration shows a ~3-fold range of variation throughout the year from 0.10 mg m^{-3} (from January to April and in October) to 0.39 mg m^{-3} (in the boreal summer). A close agreement was found between the temporal pattern followed by *in situ* and satellite derived Chl *a* data. The main mismatch between both data sets occurred early in the year, when measured values were 2-fold lower than those predicted from SeaWiFS, and in October, when the cycle predicted higher values, although the significance of this latter discrepancy should be taken with caution as it was caused by a single *in situ* measurement. Sea surface Chl *a* measured in WTRA (Fig. 5B) ranged from 0.09 mg m^{-3} (in May) to 0.37 mg m^{-3} (in November). The SeaWiFS-derived Chl *a* cycle agreed with *in situ* measured Chl *a* during boreal summer (except in August) and fall.

Seasonal variability in primary production

Simple primary production models are based in the construction of empirical relationships between depth-integrated primary production, estimated by the ^{14}C-uptake method, and sea surface Chl *a* concentration, both determined *in situ* (Behrenfeld and Falkowski, 1997). In this study, we tried this methodological approach, although being aware of the reduced data set, and found a statistically significant linear relationship between *in situ* ^{14}C-based primary production ($PO^{14}CP$) and surface Chl *a* measured during the AMT-11 cruise in the ETRA province ($PO^{14}CP = 3032.76\ Chl_{sup} - 145.45$, $r^2 = 0.94$, $n = 7$, $P < 0.001$; Fig. 6). In the WTRA province, by contrast, the relationship obtained using AMT-1, AMT-2,

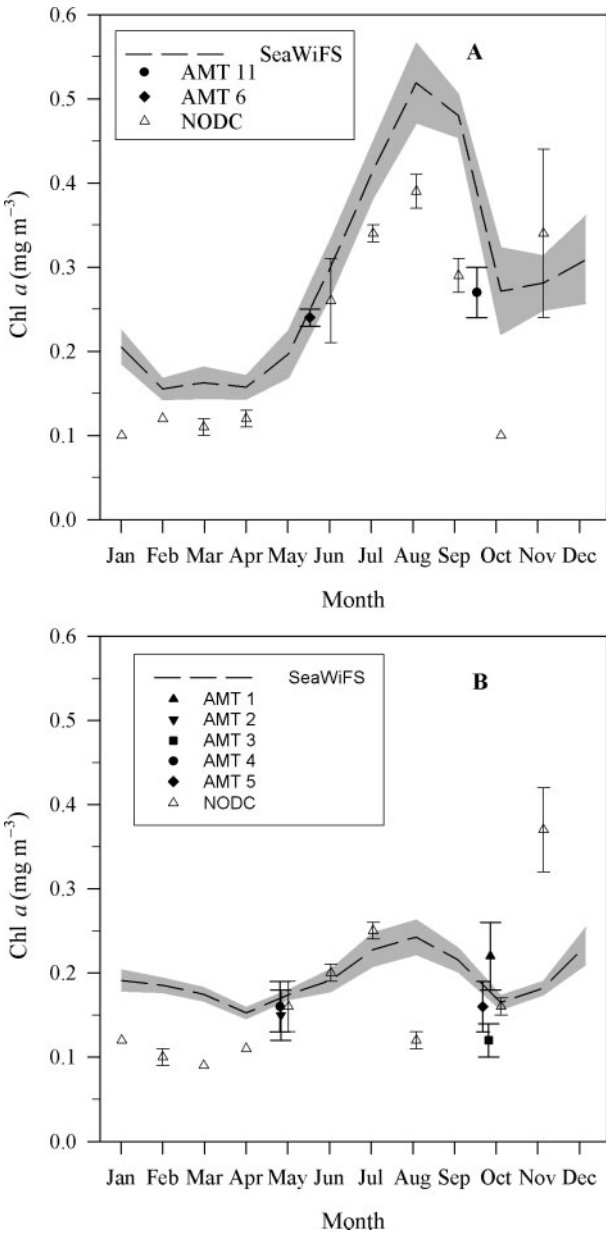

Fig. 5. Seasonal cycles of sea surface chlorophyll *a* (Chl *a*) derived from Sea-viewing Wide Field-of-view Sensor (SeaWiFS) (short dashed line) for (**A**) the box 0–10° S, 20–0° W (ETRA) and (**B**) the box 10° N–10° S, 20°–30° W (WTRA). Grey shaded area represents the standard error (SE) of SeaWiFS model. Superimposed symbols indicate the cruise-averaged (±SE) surface Chl *a* values measured during Atlantic Meridional Transect (AMT) cruises (solid symbols) and the averaged (±SE) monthly values from National Oceanographic Data Center (NODC) database (open symbols) (see Method for details).

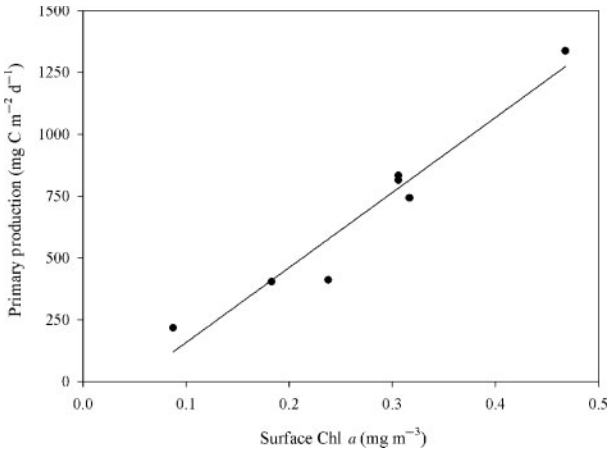

Fig 6. Empirical relationship between daily *in situ* ^{14}C-based primary production ($PO^{14}CP$) and surface chlorophyll *a* (Chl *a*) measured during the AMT-11 cruise in the ETRA province. $PO^{14}CP = 3032.76\ Chl_{sup} - 145.45$, $r^2 = 0.94$, $n = 7$, $P < 0.001$.

AMT-3, AMT-4 and AMT-5 data, was not statistically significant ($P = 0.99$), thus preventing the conversion of SeaWiFS Chl *a* into primary production in this region using our data set. The close relationship between phytoplankton Chl *a* and production found in ETRA probably resulted from the association of high depth-integrated phytoplankton carbon incorporation rates and the intensification of the equatorial upwelling. This finding contrasts with previous results suggested that the equatorial upwelling just gives rise to upward displacements of the Chl *a* maximum without actually increasing the magnitude of depth-integrated phytoplankton biomass and productivity (Herbland *et al.*, 1983, 1987).

Primary production rates estimated with our SeaWiFS-derived empirical model in part (0–10° S, 20–0° W) of the ETRA province coincided with *in situ* measured rates except in the boreal summer (Fig. 7). Thus, whereas *in situ* primary production rates showed high values in June and September, our empirical model yielded highest rates in late boreal summer. It is necessary to note that AMT-11 depth-integrated rates are included in our SeaWiFS primary production model and, consequently, they might only be used for comparative purposes with respect to other *in situ* measurements. Although the SeaWiFS model was built using 'local' AMT data, it did not correctly predict the *in situ* rates measured during boreal summer in the eastern tropical Atlantic. This may be due to the fact that the *in situ* primary production rates measured in the Equatorial Atlantic used in this study represent a limited number of observations especially when the spatial, seasonal and interannual variability observed in the Equatorial Atlantic is taken into account (Figs 1 and 2). Differences between remote sensing and ^{14}C-derived primary production rates were also reported by Campbell *et al.* (Campbell *et al.*, 2002) who compared the performance of several models and concluded that the 'best-performing algorithms were generally within a factor of two of

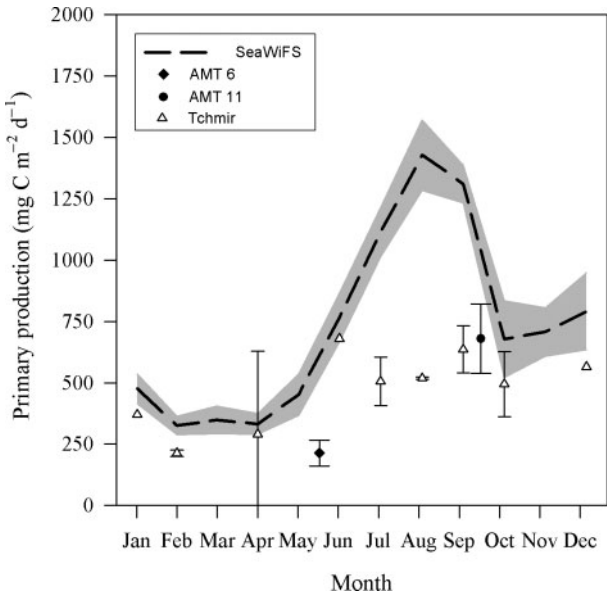

Fig. 7. Seasonal cycles of depth-integrated primary production derived from Sea-viewing Wide Field-of-view Sensor (SeaWiFS) surface chlorophyll *a* (Chl *a*) in the box 0–10° S, 20–0° W (ETRA) and an empirical Chl *a*-PP relationship obtained during the Atlantic Meridional Transect (AMT) 11 cruise (short dashed line). Grey shaded area represents the standard error of SeaWiFS model. Also shown are the average (±SE) depth-integrated primary production values measured during AMT (solid symbols) and the average (±SE) monthly values reported by Tchmir (open symbols) (see Method for details).

the ^{14}C-derived estimates'. Ducklow (Ducklow, 2003) compared primary production rates measured during Joint Global Ocean Flux Study (JGOFS) with primary production estimates reported by Longhurst (Longhurst, 1998) and found that measured values exceeded estimated ones in some biogeochemical provinces included in the Trade Winds domain (Longhurst *et al.*, 1995; Longhurst, 1998), probably as a result of the paucity of data used to build the seasonal cycles derived from CZCS.

In summary, this investigation confirms that both the magnitude and seasonality of sea surface Chl *a* are clearly different in the two locations of the ETRA and WTRA provinces, which is related to variability in SST. SeaWiFS-derived Chl *a* concentration in two areas of ETRA (0–10° S, 20–0° W) and WTRA (10° N–10° S, 20–30° W) provinces was consistent with *in situ* Chl *a* measurements carried out in the same regions. The significant empirical relationship between *in situ* ^{14}C-based primary production (PO^{14}CP) and surface Chl *a* in the ETRA province together with the SeaWiFS-derived seasonal Chl *a* cycle allowed us to derive the seasonal cycle of phytoplankton carbon incorporation rates (Fig. 7) which is largely consistent with the *in situ* measurements although it is not completely able to predict their magnitude. The annual depth-integrated primary production rate estimated for ETRA from our empirical model (1.12 Gt C year^{-1}) lies within the estimates derived from other primary production models (Eppley *et al.*, 1985; Monger *et al.*, 1997; Longhurst, 1998; Signorini *et al.*, 1999), ranging from 0.84 to 1.55 Gt C year^{-1}, and represents 12% of the open ocean primary production estimated for the Atlantic Ocean, 9.12 Gt C year^{-1}, (Longhurst *et al.*, 1995). This illustrates the significant contribution of the eastern Equatorial Atlantic to the plankton-mediated cycling of carbon at the basin scale.

ACKNOWLEDGEMENTS

This study was supported by the UK Natural Environment Research Council through the Atlantic Meridional Transect programme (grant NER/O/S/2001/00680) and by the Spanish Ministerio de Ciencia y Tecnologia (MCyT) through project CIRCANA (grant MAR1999-1072-C03-01). Comments by Alan Longhurst and two anonymous reviewers helped in improving an earlier version of the manuscript. We are indebted to the captain and crew of the *RRS James Clark Ross* for their assistance during the AMT cruises. V.P. was supported by a postgraduate fellowship from the MCyT (Spain). This is contribution number 93 of the AMT programme.

REFERENCES

Aiken, J., Rees, N. and Hooker, S. (2000) The Atlantic Meridional Transect: overview and synthesis of data. *Prog. Oceanogr.*, **45**, 257–312.

Bauerfeind, E. (1987) Primary production and phytoplankton biomass in the equatorial region of the Atlantic at 22° W. *Oceanol. Acta*, **n° sp**, 131–136.

Behrenfeld, M. J. and Falkowski, P. G. (1997) A consumer's guide to phytoplankton primary productivity models. *Limnol. Oceanogr.*, **42**, 1479–1491.

Campbell, J., Antoine, D., Armstrong, R. *et al.* (2002) Comparison of algorithms for estimating ocean primary production from surface chlorophyll, temperature, and irradiance. *Glob. Biogeochem. Cycles*, **16**, 1–15.

Carton, J. A. and Zhou, Z. (1997) Annual cycle of sea surface temperature in the Tropical Atlantic Ocean. *J. Geophys. Res.*, **102**, 27813–27824.

Colin, C., Gonella, J. and Merle, J. (1987) Equatorial upwelling at 4° W during the FOCAL program. *Oceanol. Acta*, **n°. sp**, 39–49.

Ducklow, H. W. (2003) Biogeochemical provinces: towards a JGOFS synthesis. In Fashman, M. J. R. (ed.), *Ocean Biogeochemistry: the Role of the Ocean Carbon Cycle in Global Change*. Springer-Verlag, Berlin, Heidelberg, New York.

Eppley, R. W., Stewart, E., Abbot, M. R. *et al.*, (1985) Estimating ocean primary production from satellite chlorophyll. Introduction to regional differences and statistics for the Southern California Bight. *J. Plankton Res.*, **7**, 57–70.

Garcia-Soto, C., Fernández, E., Pingree, R. D. *et al.* (1995) Evolution and structure of a shelf coccolithophore bloom in the western English Channel. *J. Plankton Res.*, **17**, 2011–2036.

Garcia-Soto, C., Sinha, B. and Pingree, R. D. (1996) Mapping a bloom of the coccolithophorid *Emiliania Huxleyi* from Airborne Thematic Mapper Data. *J. Mar. Biol. Ass. U. K.*, **76**, 839–849.

Gregg, W. W. (2002) Tracking the SeaWiFS record with a coupled physical/biogeochemical/radiative model of the global oceans. *Deep-Sea Res. II*, **49**, 81–105.

Hastenrath, S. and Merle, J. (1987) Annual Cycle of Subsurface Thermal Structure in the Tropical Atlantic Ocean. *J. Phys. Oceanogr.*, **17**, 1518–1538.

Herbland, A., Le Borgne, R., Le Bouteiller, A. *et al.* (1983) Structure hydrologique et production primaire dans l'Atlantique tropical oriental. *Océanogr. Trop.*, **18**, 249–293.

Herbland, A. and Le Bouteiller, A. (1982) The meanders of equatorial currents in the Atlantic Ocean: influence on the biological processes. *Océanogr. Trop.*, **17**, 15–25.

Herbland, A., Le Bouteiller, A. and Raimbault, P. (1987) Does the nutrient enrichment of the equatorial upwelling influence the size structure of phytoplankton in the Atlantic Ocean?. *Oceanol. Acta*, **n°. sp**, 115–120.

Herbland, A. and Voituriez, B. (1979) Hydrological structure analysis for estimating the primary production in the tropical Atlantic Ocean. *J. Mar. Res.*, **37**, 87–101.

Le Borgne, R. (1981) Relationships between the hydrological structure, chlorophyll and zooplankton biomasses in the Gulf of Guinea. *J. Plankton Res.*, **3**, 577–592.

Longhurst, A. (1993) Seasonal cooling and blooming in the tropical oceans. *Deep-Sea Res. I*, **40**, 2145–2165.

Longhurst, A. (1998) *Ecological Geography of the Sea*. Academic Press, San Diego, CA.

Longhurst, A., Sathyendranath, S., Platt, T. *et al.* (1995) An estimate of global primary production in the ocean from satellite radiometer data. *J. Plankton Res.*, **17**, 1245–1271.

Loukos, H. and Mémery, L. (1999) Simulation of nitrtae seasonal cycle in the equatorial Atlantic Ocean during 1983 and 1984. *J. Geophys. Res.*, **104**, 15549–15573.

Marañón, E., Holligan, P. M., Barciela, R. *et al.* (2001) Patterns of phytoplankton size-structure and productivity in contrasting open ocean environments. *Mar. Ecol. Prog. Ser.*, **216**, 43–56.

Marañón, E., Holligan, P. M., Varela, M. *et al.* (2000) Basin-scale variability of phytoplankton biomass, production and growth in the Atlantic Ocean. *Deep-Sea Res. I*, **47**, 825–857.

McClain, C. R. and Firestone, J. (1993) An investigation of Ekman Upwelling in the North Atlantic. *J. Geophys. Res.*, **98**, 12327–12339.

Monger, B., McClain, C. R. and Murtugudde, R. G. (1997) Seasonal phytoplankton dynamics in the eastern tropical Atlantic. *J. Geophys. Res.*, **102**, 12389–12411.

Oudot, C. (1983) La distribution des sels nutritifs (NO_3 – NO_2 – NH_4 – PO_4 – SiO_3) dans l'ocean Atlantique intertropical oriental (region du Golfe de Guinée). *Océanogr. Trop.*, **18**, 223–248.

Oudot, C. and Morin, P. (1987) The distribution of nutrients in the Equatorial Atlantic: relation to physical processes and phytoplankton biomass. *Oceanol. Acta*, **n° sp**, 121–130.

Platt, T., Caverhill, C. and Sathyendranath, S. (1991) Basin-scale estimates of oceanic primary production by remote sensing: the North Atlantic. *J. Geophys. Res.*, **96**, 15147–15159.

Rudjakov, J. A. (1997) Quantifying seasonal phytoplankton oscillations in the global offshore ocean. *Mar. Ecol. Prog. Ser.*, **146**, 225–230.

Serret, P., Fernández, E. and Robinson, C. (2002) Biogeographic differences in the net ecosystem metabolism of the open ocean. *Ecology*, **83**, 3225–3234.

Serret, P., Robinson, C., Fernández, E. *et al.* (2001) Latitudinal variation of the balance between plankton photosynthesis and respiration in the eastern Atlantic Ocean. *Limnol. Oceanogr.*, **46**, 1642–1652.

Signorini, S. R., Murtugudde, R. G., McClain, C. R. *et al.* (1999) Biological and physical signatures in the tropical and subtropical Atlantic. *J. Geophys. Res.*, **104**, 18367–18382.

Straskraba, M. and Gnauck, H. (1985) *Freshwater Ecosystems: Modelling and Simulation*. Elsevier, Amsterdam.

Tchmir, V. O. (1971) Production primaire en Atlantique Équatorial. In Rotschi, H. and Hisard, P. (eds), *Les zones productives de l'océan Atlantique Équatorial et les conditions de leur formation*. Tryd. Atlan NIRO, Kaliningrad, **37**, 175–190. Trad.

Vinogradow, M. E. (1988) Ecosystems of Equatorial upwellings. In Longhurst, A. R. (ed.), *Analysis of Marine Ecosystems*. Academic Press Limited, London.

Yoder, J. A., McClain, C. R., Feldman, G. C. *et al.* (1993) Annual Cycles of phytoplankton chlorophyll concentrations in the global ocean: a satellite view. *Glob. Biogeochem. Cycles.*, **7**, 181–193.